SUMOylation of RNF146 results in Axin degradation and activation of Wnt/β-catenin signaling to promote the progression of hepatocellular carcinoma

Dong Yin (yind3@mail.sysu.edu.cn)
Sun Yat-sen Memorial Hospital, Sun Yat-sen University https://orcid.org/0000-0002-1878-4849
Wenjia Li
Qingfang Han
The First Affiliated Hospital of Zhengzhou University
Yuanxin Zhu
Yingshi Zhou
Jingyuan Zhang
Weijun Wu
Yu Li
Long Liu
The First Affiliated Hospital of Zhengzhou University
Yuntan Qiu
Kaishun Hu
Sun Yat-Sen Memorial Hospital https://orcid.org/0000-0003-2157-6239

Article

Keywords:

Posted Date: November 10th, 2022

DOI: https://doi.org/10.21203/rs.3.rs-2212462/v1

Additional Declarations: There is **NO** conflict of interest to disclose.

Version of Record: A version of this preprint was published at Oncogene on April 7th, 2023. See the published version at https://doi.org/10.1038/s41388-023-02689-4.

SUMOylation of RNF146 results in Axin degradation and activation of Wnt/β-catenin signaling to promote the progression of hepatocellular carcinoma

Wenjia Li[1,2,9], Qingfang Han[3,4,9], Yuanxin Zhu[1,5,9], Yingshi Zhou[1,6,9], Jingyuan Zhang[1], Weijun Wu[7], Yu Li[8], Long Liu[3,4], Yuntan Qiu[1], Kaishun Hu[1]*, Dong Yin[1]*

1. Guangdong Provincial Key Laboratory of Malignant Tumor Epigenetics and Gene Regulation, Guangdong-Hong Kong Joint Laboratory for RNA Medicine, Medical Research Center, Sun Yat-Sen Memorial Hospital, Sun Yat-Sen University, Guangzhou 510120, China
2. Department of Pathology, The First Affiliated Hospital, Zhengzhou University, Zhengzhou 450052, China
3. Department of Hepatobiliary and Pancreatic Surgery, The First Affiliated Hospital of Zhengzhou University, Zhengzhou 450052, China.
4. Henan Research Centre for Organ Transplantation, The First Affiliated Hospital of Zhengzhou University, Zhengzhou 450052, China.
5. Department of Orthopedics, Sun Yat-sen Memorial Hospital of Sun Yat-sen University, Guangzhou 510120, China
6. Department of Ultrasound Sun Yat-sen Memorial Hospital, Sun Yat-sen University, Guangzhou 510120, China
7. Department of Oncology Radiotherapy, the First Affiliated Hospital, Hengyang Medical School, University of South China, Hengyang 421000, China
8. Department of Laboratory Medicine, Peking University Shenzhen Hospital, Shenzhen, China

[9]These authors contributed equally: Wenjia Li, Qingfang Han, Yuanxin Zhu, and Yingshi Zhou.

*Correspondence: Prof. D.Y., and Prof. K.S.H., Guangdong Provincial Key Laboratory of Malignant Tumor Epigenetics and Gene Regulation, Guangdong-Hong Kong Joint Laboratory for RNA Medicine, Sun Yat-Sen Memorial Hospital, Sun Yat-Sen University, Guangzhou, China 510120. Email: yind3@mail.sysu.edu.cn, huksh3@mail.sysu.edu.cn; Fax/tel: +86 20 8133 2601/+86 20 8133 2405

The authors declare no competing interests.

Abstract

Aberrant SUMOylation contributes to the progression of hepatocellular carcinoma (HCC), yet the molecular mechanisms have not been well elucidated. RNF146 is a key regulator of the Wnt/β-catenin signaling pathway, which is frequently hyperactivated in HCC. Here, it is identified that RNF146 can be modified by SUMO3. By mutating all lysines in RNF146, we found that K19, K61, K174 and K175 are the major sites for SUMOylation. UBC9/PIAS3/MMS21 and SENP1/2/6 mediated the conjugation and deconjugation of SUMO3, respectively. Furthermore, SUMOylation of RNF146 promoted its nuclear localization, while deSUMOylation induced its cytoplasmic localization. Importantly, SUMOylation promotes the association of RNF146 with Axin to accelerate the ubiquitination and degradation of Axin. Intriguingly, only UBC9/PIAS3 and SENP1 can act at K19/K175 in RNF146 and affect its role in regulating the stability of Axin. In addition, inhibiting RNF146 SUMOylation suppressed the progression of HCC both *in vitro* and *in vivo*. And, patients with higher expression of RNF146 and UBC9 have the worst prognosis. Taken together, we conclude that RNF146 SUMOylation at K19/K175 promotes its association with Axin and accelerates Axin degradation, thereby enhancing β-catenin signaling and contributing to cancer progression. Our findings reveal that RNF146 SUMOylation is a potential therapeutic target in HCC.

Introduction

The Wnt/β-catenin signaling cascade is a highly evolutionarily conserved pathway and plays fundamental roles in embryonic development, differentiation and cellular homeostasis [1]. Dysregulation of the Wnt signaling pathway has been frequently observed and implicated in multiple physiological and pathological processes, including inflammation, immunity and cancer [2-4]. Notably, aberrant Wnt/β-catenin pathway occurs in almost all stages of carcinogenesis in a cancer type-specific manner, ranging from tumour initiation

and progression to metastasis [5]. The Wnt signaling pathway is tightly and dynamically modulated via a variety of key mediators, such as β-catenin, glycogen synthase kinase-3β (GSK-3β), casein kinase 1 (CK1) and Axin [6]. Specifically, β-catenin plays a central role in the activation of Wnt signaling and its functions are precisely modulated at distinct levels through different mechanisms, including transcription control and post-translational modification. For instance, nuclear localized PHB1 binds to the Axin promoter and promotes its transcription, leading to accelerate the degradation of β-catenin and inhibition of the Wnt/β-catenin pathway [7]. Wang, et al revealed that the E3 ligase β-TrCP2 can directly mediate the neddylation of β-catenin and promote its subsequent degradation in a proteasome dependent manner [8].

It has been well documented that Axin, acting as a scaffolding protein interacts directly with APC, CK1α and GSK3 to assemble the destruction complex responsible for degradation of the substrate β-catenin [5].Importantly, the cytosolic amount of Axin directly determines the activity of the canonical Wnt pathway, and the abundance and activity of Axin are tightly and precisely modulated by several mechanisms, including ubiquitination, methylation and poly(ADP-ribosyl)ation [7, 9, 10]. For instance, the HECT-type E3 ubiquitin ligase Smurf1 promotes K29-linked polyubiquitination of Axin and disrupts the interaction of Axin with LRP5/6, leading to attenuation of the Wnt/β-catenin signaling [11]. Tankyrase-mediated PARylation of Axin also contributes to the regulation of Axin protein stability via recruitment of the PARylation-dependent E3 ligase RNF146, subsequently resulting in stabilization of β-catenin and activation of Wnt/β-catenin signaling [12-14]. In addition, deubiquitination processes mediated by deubiquitinases (DUBs) have also been well established in the regulation of Axin protein stability [15]. Cong, et al showed that the DUB USP7 can directly bind to Axin and reduce its ubiquitination level and increase its stability, thereby regulating cell differentiation by reducing Wnt/β-catenin signaling [16]. Therefore, the precise modulation of Axin turnover is crucial for controlling the activation of the Wnt pathway, and an

aberrant decrease in the Axin abundance leads to over-activate of the Wnt-β-catenin signaling pathway and tumorigenesis. However, much remains to be done to obtain a clear understanding of the mechanisms by which for the precise regulation of the abundance of Axin is precisely regulated.

SUMOylation is a highly dynamic and reversible post-translational modification characterized by covalent conjugation of small ubiquitin-like modifier (SUMO) moieties to substrates at specific lysine residues, and it participates in a variety of cellular processes, including DNA repair and replication, cell cycle transition, cell metabolism and antitumour immune responses [17-19]. Accumulating evidence has indicated that the SUMOylation pathway is constitutively upregulated and highly activated in multiple cancer types, such as hepatocellular carcinoma, pancreatic ductal adenocarcinoma and lymphomas [20]. Dysregulation of SUMOylation signaling accelerates tumorigenesis and tumour progression by regulating cell cycle progression-related, angiogenic, and metabolic pathways as well as immune tolerance [21-25]. Therefore, it is reasonable that targeting the SUMOylation pathway may provide a promising therapeutic strategy for cancer, and several SUMOylation inhibitors have been developed and approved for use in clinical trials. Notably, SUMOylation is also implicated in the modulation of Wnt/β-catenin signaling. For instance, SUMOylation of TBL1-TBLR1 blocked it from interacting with the nuclear receptor corepressor (NCoR) complex and increased the binding affinity of the TBL1-TBLR1-β-catenin complex for the promoter of Wnt downstream genes, thereby leading to activation of the Wnt signaling pathway [26]. In addition, the deSUMOylase SENP7S can recognize both SUMOylated β-catenin and SUMOylated Axin, and can maintain the interaction of these complexes, thereby promoting ubiquitylation-dependent degradation of β-catenin and inhibiting the activation of the Wnt/β-catenin pathway [27].

RNF146 is a PARylation-dependent E3 ubiquitin ligase and involved in a variety of cellular processes and signal transduction pathways, including

TNKS1/2-mediated activation of the Wnt-β-catenin and Hippo-YAP pathways, as well as TNF-induced activation of cell death pathways [10, 13, 28]. Structurally, the E3 ligase RNF146 is composed of two well-characterized domains, the RING domain responsible for transferring ubiquitin moieties to substrates and the WWE domain mediating the recognition of PARylated substrates by RNF146 [13]. Hence, RNF146 plays critical roles in PARP1/2 and TNKS1/2 mediated cellular processes. For instance, RNF146 can recognize PTEN modified by TNKS1/2-mediated PARylation and promote its ubiquitination and degradation in a proteasome-dependent manner, thereby resulting in activation of the PI3K-AKT pathway and cell proliferation[29]. Our previous study also revealed that RNF146 can recognize and interact with BRD7 modified by PARP1-induced PARylation and target this protein for degradation through the ubiquitin-proteasome pathway, leading to activation of AKT phosphorylation and resistance of cancer cells to chemotherapy [30]. Moreover, aberrant expression of RNF146 is frequently observed in multiple cancer types, including colorectal cancer and lung cancer [31, 32]. For example, the protein level of RNF146 in non-small cell lung cancer (NSCLC) tissues is positively correlated with nuclear expression of β-catenin, and overexpression of RNF146 promotes NSCLC cell proliferation and invasiveness through the classical Wnt/β-catenin pathway, thereby predicting poor prognosis in NSCLC patients [33]. However, the biological function and clinical significance of RNF146 in hepatocellular carcinoma remain unknown.

In the current study, we found that RNF146, a key E3 ubiquitin ligase modifying Axin, can be SUMOylated by SUMO3, thereby reducing the stability of Axin and activating β-catenin signaling to promote the progression of HCC. Specifically, PIAS3 and SENP1 mediate the SUMOylation and deSUMOylation, respectively, of RNF146 at lysine19 and lysine 175. Moreover, SUMOylation promotes the association of RNF146 and Axin, leading to increased ubiquitination and degradation of Axin. Our findings emphasized that targeting RNF146 SUMOylation might be a promising therapeutic strategy for HCC.

MATERIALS AND METHODS

Cell culture and transfection

HeLa and HEK293T cells were obtained from ATCC (Manassas, VA, USA). SK-hep1 cells were provided by the Stem Cell Bank of the Chinese Academy of Sciences (Shang Hai, China), and HCC-LM3 cells were a gift from Prof. Peng Li (Sun Yat-Sen University Memorial Hospital, Guangzhou, China). All cells were cultured in DMEM (Thermo Fisher Scientific, USA) containing 10% fetal bovine serum (FBS, LONSERA) in 5% CO2 at 37°C. The Mycoplasma PCR Detection Kit (Sigma, USA) was routinely employed to exclude mycoplasma contamination. STR profiling was performed for authentication of all cell lines. Plasmid transfection was performed using Viafect (Promega, USA). siRNA transfection was performed using Lipofectamine RNAiMAX (Thermo Fisher Scientific, USA) according to the manufacturer's protocol. The sequences of the indicated siRNAs are shown in Supplementary Table S1.

Antibodies and reagents

The antibodies and reagents used in this paper are listed in Supplementary Table S2.

Plasmid construction and stable cell line establishment

For plasmid construction, full-length cDNAs coding for RNF146, SUMO1/2/3, SENP1/2/3/5/6/7, PIAS1/2/3/4, and MMS21 were obtained from human HEK293 cells by RT-PCR. Then, cDNAs coding for SUMO1/2/3, SENP1/2/3/5/6/7, PIAS1/2/3/4, and MMS21 were inserted into the pcDNA3.1 vector after amplification with the indicated primers. In addition, cDNAs coding for RNF146, SENP1/2/6, PIAS3 and MMS21 were constructed using Gateway technology as described previously [52] (Invitrogen, USA). The related K-to-R mutants of SFB-RNF146 were cloned into the destination vector using the a TaKaRa MutanBEST Kit (TaKaRa, Japan). To establish the RNF146-knockout cell line, RNF146 CRISPR vectors (Santa Cruz Biotechnology, USA) were

transiently transfected into SK-hep1 and HCC-LM3 cells, prior to puromycin treatment for 48 hours. After selection, the cells were harvested by trypsinization and cultured to obtain clones. Several clones were picked, cultured and validated by Western blot analysis. All constructed plasmids are listed in Supplementary Table S3.

Statistics

All statistical results are shown as the mean ± SDs. Student's t test or one-way ANOVA were performed with GraphPad Prism 8.0 or SPSS 22.0 software. Differences with $p< 0.05$ were considered to be statistically significant (n. s, not significant; *$p < 0.05$; **$p < 0.01$; ***$p < 0.001$).

Additional methods are presented in the Supporting Information.

Results

RNF146 is SUMOylated by SUMO3 at K19, K61 and K174/175

To determine whether RNF146 is subjected to covalent SUMO modification, we transiently transfected SUMO1, SUMO2, or SUMO3 into HeLa cells. As shown in Fig. 1A, RNF146 was modified strongly by SUMO3 but only moderately by SUMO1/2 (Fig. 1A, B). It has been reported that UBC9, the sole SUMO-conjugating enzyme for SUMOylation, directly recognizes the SUMO consensus motif (SCM) and selects substrate lysines for modification [34, 35]. Thus, we tested whether the SUMOylation of RNF146 can be modulated by UBC9. As expected, depletion of endogenous UBC9 profoundly decreased SUMO3 conjugation to RNF146 (Fig. 1C). Moreover, inhibiting endogenous UBC9 using the inhibitor 2-D08 significantly reduced the SUMOylation level of RNF146 (Fig. 1D). Collectively, these data indicated that RNF146 was efficiently modified by SUMO3 in vivo.

Furthermore, we identified the SUMOylation site(s) in RNF146. There are thirteen lysine (K) residues, K19, K52, K61, K68, K84, K94, K130, K132, K133, K164, K166, K174 and K175, in the RNF146 protein. To identify all potential

lysine site(s) at which RNF146 is SUMOylated, a series of plasmids expressing RNF146 with mutation of these lysine (K) residues to arginine (R) mutations were constructed and cotransfected with HA-SUMO3 into HeLa cells. As shown in Fig 1E, the SUMOylation levels of the K19R, K61R and K174/175R mutants were significantly decreased compared with those of wild-type RNF146. Moreover, the K19, K61 and K174/175 residues of RNF146 are highly conserved among various species (Fig. 1F). These results strongly supported the idea that the conjugation of SUMO3 to RNF146 occurs mainly at K19, K61 and K174/175.

PIAS3 and MMS21 are the dominant SUMO E3 ligases for RNF146

Next, we sought to identify the SUMO E3 ligase responsible for the SUMOylation of RNF146. Previous studies have revealed that PIAS family members, including PIAS1, PIAS2α, PIAS3, and PIAS4, as well as the methyl methanesulfonate-sensitivity protein MMS21/Nse2, are the major "writers" mediating substrate SUMOylation [36, 37]. Therefore, constructs expressing PIAS family members and MMS21 were cotransfected individually with the RNF146 plasmid into HeLa cells and a co-IP assay was performed. As shown in Fig. 2A and B, PIAS3 and MMS21 but not PIAS1, PIAS2α and PIAS4 specifically associated with RNF146, leading to upregulation of RNF146 SUMOylation. Furthermore, the association between RNF146 with MMS21 or PIAS3 were clearly detected at the corresponding endogenous levels (Fig. 2C). In addition, immunofluorescence staining combined with a proximity labelling approach was employed to detect the colocalization of RNF146 with PIAS3 or MMS21 in SK-hep1 and 293T cells. Both PIAS3 and MMS21 colocalized with RNF146. Importantly, PIAS3 and MMS21 promoted the nuclear localization of RNF146 while reducing its cytoplasmic distribution (Fig. 2D and Supplementary Fig. S1A). Consistent with this finding, depletion of either endogenous PIAS3 or MMS21 greatly inhibited RNF146 SUMOylation (Fig. 2E, F). Double depletion of endogenous PIAS3 and MMS21 dramatically reduced

RNF146 SUMOylation (Fig. 2G). Taken together, these results suggest that PIAS3 and MMS21 are the primary SUMO E3 ligases for RNF146.

SENP1/2/6 are the dominant deSUMOylase responsible for removing SUMOylation from RNF146

It has been documented that SUMOylation is a highly dynamic and reversible process and that deSUMOylation is accomplished by SENP family members, namely, SENP1, 2, 3, 5, 6 and 7, in human cells [38, 39]. To determine which SENP catalyses the deSUMOylation of RNF146, we cotransfected SENP constructs individually with the RNF146 plasmid into HeLa cells and performed co-IP assays. As shown in Fig. 3A, SENP1/2/6 but not SENP3/5/7 specifically interacted with RNF146 and greatly reduced the SUMOylation levels of RNF146. Moreover, these interactions were further confirmed by a reciprocal co-IP assay using anti-MYC beads (Fig. 3B). Furthermore, the endogenous complex containing RNF146 and SENP1, SENP2 or SENP6 were also detected by a co-IP using an anti-RNF146 antibody (Fig. 3C). Moreover, TurboID-based proximity labelling revealed that SENP1 promoted the cytoplasmic translocation of RNF146 and was primarily colocalized with RNF146 in the cytoplasm (Fig. 3D). However, both SENP2 and SENP6 enhanced the nuclear accumulation of RNF146 and formed discrete nuclear puncta exhibiting obvious colocalization with RNF146 (Supplementary Fig. S2A). Consistent with this observation, depletion of endogenous SENP1, SENP2 and SENP6 markedly increased the SUMOylation level of RNF146 (Fig. 3E and Supplementary Fig. S2B-C). Triple depletion of endogenous SENP1, SENP2, and SENP6 further enhanced the level of RNF146 SUMOylation compared with that in cells with depletion of SENP1, SENP2 or SENP6 alone (Fig. 3F). Taken together, these results indicate that SENP1/2/6 are the bona fide deSUMOylases of RNF146.

SUMOylation of RNF146 at lysine 19 and lysine 175 promotes the

interaction of RNF146 with Axin and the degradation of Axin

It has been reported that Axin is a scaffolding protein in the β-catenin destruction complex and that its stability is regulated by RNF146 [10, 40]. However, the molecular mechanism by which RNF146 regulates Axin degradation remains unknown. Considering the pivotal role of aberrant Wnt/β-catenin signaling in HCC progression, we sought to determine whether SUMOylation modulates the role of RNF146 in regulating Axin degradation and promotes HCC progression. As shown in Fig. 4A, knocking out endogenous RNF146 significantly increased the protein level of Axin, accompanied by downregulation of β-catenin, and these effects were reversed by reintroducing SFB-RNF146-WT. Interestingly, reintroduction of RNF146-K19R or RNF146-K175R failed to reverse the change caused by knocking out endogenous RNF146, but reintroduction of RNF146-K61R or RNF146-K174R did reverse these changes (Fig. 4A). Thus, SUMOylation at K19/K175 but not SUMOylation at K61/K174 contributes to the function of RNF146 in the degradation of Axin. As β-catenin signaling is negatively regulated by Axin and the nuclear localization of β-catenin determines its activity, we further investigated the effect of RNF146 SUMOylation on β-catenin signaling. We found that overexpressing RNF146-WT but not RNF146-K19R or RNF146-K175R in SK-hep1 cells significantly increased the protein level of β-catenin in the nucleus but only slightly increased the protein level of β-catenin in the cytoplasm (Fig. 4B, C). Then, the enzymes mediating the SUMOylation and deSUMOylation of RNF146 were knocked out. Strikingly, silencing PIAS3 but not MMS21 severely blocked RNF146-induced β-catenin accumulation while upregulating the expression of Axin (Fig. 4D). Additionally, silencing SENP1 but not SENP2 or SENP6 dramatically decreased Axin expression and increased β-catenin expression (Fig. 4E).

GSK-3β phosphorylates Ser33, Ser37 and Thr41 in β-catenin to promote its degradation and inhibit Wnt signaling [41]. On the other hand, phosphorylation of β-catenin at Ser675 promotes its interaction with various transcription

311 factors such as TCF4 and TBP [42]. To investigate whether SUMOylation of
312 RNF146 is involved in regulating Axin stability and Wnt signaling in HCC cells,
313 we depleted endogenous UBC9 to impair RNF146 SUMOylation. Consistent
314 with previous observation, depletion of UBC9 decreased the total β-catenin
315 level and blocked β-catenin signaling as shown by the increased
316 phosphorylation of β-catenin at S33/S37/T41 and reduced phosphorylation on
317 S675 (Supplementary Fig. S3A). Importantly, the abolition of RNF146
318 SUMOylation stabilized Axin by decreasing its ubiquitination (Supplementary
319 Fig. S3A). Previous studies have shown that SUMOylation alters the stability
320 or protein-protein interactions of the target proteins [23]. We found that
321 mutation of RNF146 had little effect on the total protein level and protein
322 half-life compared with those of RNF146-WT (Supplementary Fig. S3B). Thus,
323 we speculated that SUMOylation of RNF146 might influence the association of
324 RNF146 with its substrate Axin. Indeed, mutation of either K19 or K175
325 severely interfered with the RNF146-Axin interaction (Fig. 4F). Moreover, the
326 K19 and K175 mutations of RNF146 failed to mediate the ubiquitination of Axin
327 (Fig. 4G). Additionally, through sequence alignment, we identified a
328 SUMO-interacting motifs (SIMs) in Axin, which were conserved among multiple
329 species (Supplementary Fig. S3C). Collectively, these results indicate that
330 PAIS3 and SENP1 mediate RNF146 SUMOylation and deSUMOylation at K19
331 and K175, which is critical for the RNF146-Axin interaction and the subsequent
332 the degradation of Axin.
333
334 **RNF146 SUMOylation activates β-catenin signaling and promotes the**
335 **proliferation of HCC cells in vitro**
336 As both β-catenin signaling and SUMOylation play an important role in the
337 progression of cancer especially in HCC, we sought to determine whether
338 RNF146 SUMOylation can modulate β-catenin signaling in HCC and
339 contribute to HCC progression. First, RNF146 was overexpressed in SK-hep1
340 and HCC-LM3 HCC cells. Indeed, RNF146 downregulated Axin and

decreased the S33/S37/T41 phosphorylation but increased the S675 phosphorylation of β-catenin, indicating the activation of Wnt signaling (Fig. 5A). Conversely, knocking down or depleting RNF146 with siRNAs or sgRNAs promoted β-catenin phosphorylation at S33/S37/T41 while reducing its phosphorylation at Ser675 (Fig. 5B and Supplementary Fig. S4A). Next, we validated the role of RNF146 in the progression of HCC. The colony formation assay showed that overexpressing or depleting RNF146 significantly promoted or inhibited HCC cell proliferation, respectively (Fig. 5C, D and Supplementary Fig. S4B and S4C). It has been reported that β-catenin activation contributes to the G1-S transition and counteracts the increased level of replication stress in cancer cells [43, 44]. Thus, a DNA fiber assay was performed and the results showed that overexpression of RNF146 markedly increased but depletion of RNF146 significantly decreased the replication fork speed in HCC cells (Fig. 5E, F and Supplementary Fig. S4D and S4E). Taken together, these results suggest that RNF146 promotes the activation of β-catenin signaling and the subsequent progression of HCC.

Furthermore, we sought to validate whether the tumour-promoting function of RNF146 depends on its SUMOylation at K19 and K175. We found that reducing RNF146 SUMOylation by knocking down PIAS3 significantly inhibited the proliferation of HCC cells. In addition, combined depletion of PIAS3 and RNF146 further augmented the cell growth inhibition caused by knocking down RNF146 alone (Supplementary Fig. S4F). To directly determine the role of RNF146 SUMOylation in the progression of HCC, a series of cell lines with stable depletion of endogenous RNF146 and reintroduction of control vector, the wild-type RNF146 plasmid or RNF146 mutant plasmids were generated (Supplementary Fig. S4G). The BrdU incorporation and *c*olony formation assays showed that RNF146 depletion significantly suppressed the proliferation of HCC cells, which was completely rescued by reintroduction of RNF146-WT but not RNF146-K19R or RNF146-K175R (Fig. 5G, H and Supplementary Fig. S4H and S4I). Moreover, the DNA fiber assay showed that

RNF146-K19R and RNF146-K175R failed to rescue the RNF146 depletion-induced replication fork stress in HCC cells (Fig. 5I, J). Collectively, these results indicate that SUMOylation of RNF146 at K19 and K175 is essential for its role in the progression of HCC cells.

Abolishing RNF146 SUMOylation inhibits HCC tumorigenesis

To further confirm the function of RNF146 SUMOylation in the progression of HCC in vivo, SK-hep1 cell lines with stable depletion of endogenous RNF146 and reintroduction of wild-type RNF146, RNF146-K19R or RNF146-K175R were used. The results showed that RNF146-WT but not RNF146-K19R or RNF146-K175R significantly promoted xenograft tumour growth (Fig. 6A-C). In addition, we measured the expression of Axin and β-catenin, and found that RNF146-WT but not RNF146-K19R or RNF146-K175R downregulated the expression of Axin and increased the expression of β-catenin (Fig. 6D). Consistent with these findings, RNF146-WT, but not RNF146-K19R or RNF146-K175R promoted the expression of Ki67 (Fig. 6E). Thus, SUMOylation of RNF146 is vital for its role in HCC progression in vivo. As shown earlier, the SUMOylation inhibitor 2-D08 significantly blocked RNF146 SUMOylation (Fig. 1D), and we then determined whether targeting SUMOylation can inhibit the progression of HCC. The results showed that the proliferative capacity of SK-hep1 and HCC-LM3 cells was decreased by 2-D08 treatment in vitro (Supplementary, Fig. S5A and S5B). In addition, 2-D08 reduced xenograft tumour growth, with only weak toxicity (Fig. 6F, G and Supplementary Fig. S5C and S5D). Moreover, the protein level of Axin was increased, while the protein level of β-catenin and number of Ki-67 positive cells were decreased in tumour xenografts from mice treated with 2-D08 (Supplementary Fig. S5E and S5F). Collectively, these results confirm that RNF146 SUMOylation plays a pivotal role in the progression of HCC and could serve as a therapeutic target in HCC.

The clinical significance of RNF146 SUMOylation/Axin/β-catenin axis in human HCC tissues

To determine the clinical significance of RNF146 SUMOylation/Axin/β-catenin signaling axis, we analyzed the expression of Axin, RNF146 and enzymes mediating RNF146 SUMOylation in tissues of HCC patients. In addition to the low expression of Axin, we found that PIAS3 and UBC9 were significantly upregulated, while SENP1 and Axin were obviously downregulated in 12 HCC tissues, compared with paracancerous tissues (Fig. 7A, B and Supplementary Fig. S6A and S6B). RNF146 was higher expressed in 5/12 HCC tissues, yet no significantly change was examined, consistent with its expression in public database GEPIA2 (http://gepia2.cancer-pku.cn/) and CPTAC (http://ualcan.path.uab.edu/index.html) (Fig. 7A, B and Supplementary Fig. S6C). Nonetheless, by performing immunohistochemistry (IHC) analysis in 99 HCC tissues, it was showed that the expression of RNF146 was positively correlative with Axin expression. Additionally, the expression of UBC9 and PIAS3 was positively correlative with Axin expression, whereas SENP1 was negatively correlated with Axin expression (Fig. 7C, D). By using the public database GEPIA2 and CPTAC, we found that the mRNA and protein level of UBC9 are significantly overexpressed in HCC specimens and its high expression is correlated with poor prognosis of HCC patients (Fig. 7E and Supplementary Fig. S6D and S6E). Also, the expression of UBC9 is positively correlative with the expression of RNF146 and β-catenin target genes such as MMP7, CD44 and MYC (Supplementary Fig. S6F). More importantly, HCC patients with high expression of both RNF146 and UBC9 have the worst prognosis (Fig. 7F). These results imply that SUMOylation might play an important role in HCC progression and RNF146 might be a key downstream target of SUMOylation. Taken together, these data provide strong evidences that SUMOylation cooperates with RNF146 to downregulate the expression of Axin, promote the activation of β-catenin signaling and contribute to the poor prognosis of HCC patients (Fig. 8).

Discussion

In the current study, we found that RNF146 can be modified by SUMO3 and that PIAS3 and SENP1 mediate the SUMOylation and de-SUMOylation of RNF146, respectively. In particular, SUMOylation of RNF146 at K19/K175 controls its interaction with Axin. By accelerating the ubiquitination and degradation of Axin, RNF146 SUMOylation activates Wnt/β-catenin signaling and contributes to the progression of HCC. Our study emphasizes that targeting SUMOylation might be a promising therapeutic strategy for cancer.

SUMOylation has been identified in thousands of proteins and is involved in a variety of physiological and pathological processes. However, only a few enzymes are known to mediate the reversible conjugation-deconjugation of SUMO moieties to target proteins [39]. Herein, we found that the E3 ubiquitin ligase RNF146 is predominantly modified by SUMO3, whose conjugation is catalyzed by PIAS3 and MMS21 and whose deconjugation is catalyzed by SENP1/2/6. Of note, the Ψ-K-x-E/D (where Ψ represents a hydrophobic residue) motif is proposed to be the most common consensus motif for SUMOylation on target substrates [45, 46]. However, only half of all SUMOylation sites precisely follow this pattern, and SUMOylation can occur at other lysine residues [47, 48]. Thus, we mutated all lysines in RNF146 and, consistent with these previous findings, K19, K61, K174 and K175 could be modified by SUMO3, and three of these lysines (K19, K61, K174) did not conform to the above consensus motif. Previous studies have shown that both E3 ligases and SENPs are substrate specific and cannot compensate for each other [17, 39]. Thus, we speculate that distinct enzymes might mediate SUMOylation at different lysines in RNF146 and subsequently play different roles. RNF146 binds directly to and ubiquitinates Axin, thereby accelerating its degradation[10]. Interestingly, we found that only PIAS3 and SENP1 can act at K19/K175 in RNF146 and affect the ubiquitination and stability of Axin, while mutation of K61 or K174 had no effect on the association between RNF146

and Axin. Thus, our findings add a new layer of complexity to the SUMOylation machinery.

SUMOylation plays a pivotal role in orchestrating the activity, stability, localization, protein–protein interactions and, ultimately, the function of target proteins, thereby mediating a variety of cellular processes. We found that SUMOylation of RNF146 promotes its nuclear localization and association with Axin without influencing its stability. Conversely, deSUMOylation of RNF146 induces its cytoplasmic localization. It has been reported that RNF146 interacts with and ubiquitinates Axin with tankyrase-mediated PARsylation and promotes Wnt signaling by contributing to the degradation of Axin [10]. Here, our study showed that SUMOylation of RNF146 increased its association with Axin and promoted the ubiquitination and degradation of Axin, which in turn inhibited the degradation of β-catenin and promoted Wnt signaling. It has been proposed that SUMO is localized predominantly in the nucleus [39]. Considering that Axin is a nuclear-cytoplasmic shuttling protein and that endogenous tankyrase is localized mainly in the nucleus [49, 50], it is conceivable that PIAS3-mediated SUMOylated RNF146 might interact with and ubiquitinate PARsylated Axin in the nucleus. In addition, K61/K174 in RNF146 could be SUMOylated, and MMS21 together with SENP2/6 could modify the SUMOylation and localization of RNF146. Unlike the diffuse distribution of RNF146 in the nucleus induced by PIAS3, MMS21 was colocalized with RNF146 as scattered puncta throughout the nucleus, implying that MMS21 might SUMOylate RNF146 to play different roles. RNF146 is an E3 ubiquitin ligase and has multiple substrates, such as BRD7 and SH3BP5 [30, 51]. As our group and other groups have reported, both BRD7 and MMS21 participate in DNA repair [52, 53]; thus, the function of BRD7-mediated RNF146 SUMOylation and whether this SUMOylation occurs at K61/K174 will be elucidated in the future.

Overall, we revealed that reversible SUMOylation of RNF146 at K19/K175 plays a pivotal role in its localization and functional regulation. Mechanistically,

SUMOylation of RNF146 promotes its association with Axin and subsequently accelerates the degradation of Axin, thereby enhancing β-catenin signaling and contributing to cancer progression (Fig. 6G). Our study revealed a new layer of regulation upstream of the RNF146-Axin-β-catenin axis and indicating that inhibiting the SUMOylation of RNF146 could serve as a proposing therapeutic strategy for HCC.

ACKNOWLEDGMENTS

This study was funded by grants from the National Key Research and Development Program of China (2021YFA0909300 to D.Y.), the Natural Science Foundation of China (82073067, 81872140, 81621004, and 81420108026 to D.Y. 82172636 to KS.H.); Guangdong Science and Technology Department (2019B020226003, 2021A0505030084, 2020B1212060018, and 2020B1212030004 to D.Y.); The Key R & D and promotion in Henan Province (212102310114 to QF.H.).

AUTHOR CONTRIBUTIONS

Research conception and design: D.Y., KS.H., WJ.L., QF.H.; Experimental of methodology: KS.H., WJ.L., YX.Z., Y.L., WJ.W.; Acquisition of data (provided animals, patient samples and provided facilities, etc.): QF.H., JY.Z.,YS.Z.; Analysis and interpretation of data (e.g., statistical analysis, biostatistics, computational analysis): KS.H., WJ.L., QF.H., YX.Z, Y,L., YS.Z, YT.Q.; Write manuscript: KS.H., WJ.L., QF.H.; Technical, or material support (e.g., organizing data, constructing databases,): QF.H., L.L., KS.H.

COMPETING INTERESTS

The authors declare no competing interests.

ETHICS

This study was approved by the Animal Research Committee of Sun Yat-sen

University Cancer Center. Ethical approval was obtained from the Ethics Committee of Sun Yat-sen Memorial Hospital (Guangzhou, China).

References

1. Albrecht LV, Tejeda-Muñoz N, De Robertis EM. Cell Biology of Canonical Wnt Signaling. Annu Rev Cell Dev Biol. 2021; 37: 369-389.
2. Gao Q, Zhu H, Dong L, Shi W, Chen R, Song Z *et al*. Integrated Proteogenomic Characterization of HBV-Related Hepatocellular Carcinoma. Cell. 2019; 179: 561-577 e522.
3. Zhang Y, Chen F, Chandrashekar DS, Varambally S, Creighton CJ. Proteogenomic characterization of 2002 human cancers reveals pan-cancer molecular subtypes and associated pathways. Nat Commun. 2022; 13: 2669.
4. Parsons MJ, Tammela T, Dow LE. WNT as a Driver and Dependency in Cancer. Cancer Discov. 2021; 11: 2413-2429.
5. Liu J, Xiao Q, Xiao J, Niu C, Li Y, Zhang X *et al*. Wnt/beta-catenin signalling: function, biological mechanisms, and therapeutic opportunities. Signal Transduct Target Ther. 2022; 7: 3.
6. Yu F, Yu C, Li F, Zuo Y, Wang Y, Yao L *et al*. Wnt/beta-catenin signaling in cancers and targeted therapies. Signal Transduct Target Ther. 2021; 6: 307.
7. Jackson DN, Alula KM, Delgado-Deida Y, Tabti R, Turner K, Wang X *et al*. The Synthetic Small Molecule FL3 Combats Intestinal Tumorigenesis via Axin1-Mediated Inhibition of Wnt/beta-Catenin Signaling. Cancer Res. 2020; 80: 3519-3529.
8. Wang B, Wang T, Zhu H, Yan R, Li X, Zhang C *et al*. Neddylation is essential for beta-catenin degradation in Wnt signaling pathway. Cell Rep. 2022; 38: 110538.
9. Schaefer KN, Peifer M. Wnt/Beta-Catenin Signaling Regulation and a Role for Biomolecular Condensates. Dev Cell. 2019; 48: 429-444.
10. Zhang Y, Liu S, Mickanin C, Feng Y, Charlat O, Michaud GA *et al*. RNF146 is a poly(ADP-ribose)-directed E3 ligase that regulates axin degradation and Wnt signalling. Nat Cell Biol. 2011; 13: 623-629.
11. Fei C, Li Z, Li C, Chen Y, Chen Z, He X *et al*. Smurf1-mediated Lys29-linked nonproteolytic polyubiquitination of axin negatively regulates Wnt/β-catenin signaling. Molecular and cellular biology. 2013; 33: 4095-4105.
12. Croy HE, Fuller CN, Giannotti J, Robinson P, Foley AVA, Yamulla RJ *et al*. The Poly(ADP-ribose) Polymerase Enzyme Tankyrase Antagonizes Activity of the β-Catenin Destruction Complex through ADP-ribosylation of Axin and APC2. The Journal of biological chemistry. 2016; 291: 12747-12760.
13. DaRosa PA, Wang Z, Jiang X, Pruneda JN, Cong F, Klevit RE *et al*. Allosteric activation of the RNF146 ubiquitin ligase by a poly(ADP-ribosyl)ation signal. Nature. 2015; 517: 223-226.
14. Morrone S, Cheng Z, Moon RT, Cong F, Xu W. Crystal structure of a Tankyrase-Axin complex and its implications for Axin turnover and Tankyrase substrate recruitment. Proceedings of the National Academy of Sciences of the United States of America. 2012; 109: 1500-1505.
15. Han W, Koo Y, Chaieb L, Keum BR, Han JK. UCHL5 controls beta-catenin destruction complex function through Axin1 regulation. Sci Rep. 2022; 12: 3687.

16. Ji L, Lu B, Zamponi R, Charlat O, Aversa R, Yang Z *et al*. USP7 inhibits Wnt/beta-catenin signaling through promoting stabilization of Axin. Nat Commun. 2019; 10: 4184.
17. Zhou L, Zheng L, Hu K, Wang X, Zhang R, Zou Y *et al*. SUMOylation stabilizes hSSB1 and enhances the recruitment of NBS1 to DNA damage sites. Signal Transduct Target Ther. 2020; 5: 80.
18. Lin Q, Yu B, Wang X, Zhu S, Zhao G, Jia M *et al*. K6-linked SUMOylation of BAF regulates nuclear integrity and DNA replication in mammalian cells. Proc Natl Acad Sci U S A. 2020; 117: 10378-10387.
19. Yang W, Robichaux WG, 3rd, Mei FC, Lin W, Li L, Pan S *et al*. Epac1 activation by cAMP regulates cellular SUMOylation and promotes the formation of biomolecular condensates. Science advances. 2022; 8: eabm2960.
20. Seeler JS, Dejean A. SUMO and the robustness of cancer. Nat Rev Cancer. 2017; 17: 184-197.
21. Kumar S, Schoonderwoerd MJA, Kroonen JS, de Graaf IJ, Sluijter M, Ruano D *et al*. Targeting pancreatic cancer by TAK-981: a SUMOylation inhibitor that activates the immune system and blocks cancer cell cycle progression in a preclinical model. Gut. 2022.
22. Li J, Xu Y, Long XD, Wang W, Jiao HK, Mei Z *et al*. Cbx4 governs HIF-1alpha to potentiate angiogenesis of hepatocellular carcinoma by its SUMO E3 ligase activity. Cancer Cell. 2014; 25: 118-131.
23. Shangguan X, He J, Ma Z, Zhang W, Ji Y, Shen K *et al*. SUMOylation controls the binding of hexokinase 2 to mitochondria and protects against prostate cancer tumorigenesis. Nat Commun. 2021; 12: 1812.
24. Nakamura A, Grossman S, Song K, Xega K, Zhang Y, Cvet D *et al*. The SUMOylation inhibitor subasumstat potentiates rituximab activity by IFN1-dependent macrophage and NK cell stimulation. Blood. 2022; 139: 2770-2781.
25. Demel UM, Boger M, Yousefian S, Grunert C, Zhang L, Hotz PW *et al*. Activated SUMOylation restricts MHC class I antigen presentation to confer immune evasion in cancer. J Clin Invest. 2022; 132.
26. Choi HK, Choi KC, Yoo JY, Song M, Ko SJ, Kim CH *et al*. Reversible SUMOylation of TBL1-TBLR1 regulates β-catenin-mediated Wnt signaling. Molecular cell. 2011; 43: 203-216.
27. Karami S, Lin FM, Kumar S, Bahnassy S, Thangavel H, Quttina M *et al*. Novel SUMO-Protease SENP7S Regulates beta-catenin Signaling and Mammary Epithelial Cell Transformation. Sci Rep. 2017; 7: 46477.
28. Liu L, Sandow JJ, Leslie Pedrioli DM, Samson AL, Silke N, Kratina T *et al*. Tankyrase-mediated ADP-ribosylation is a regulator of TNF-induced death. Science advances. 2022; 8: eabh2332.
29. Li N, Zhang Y, Han X, Liang K, Wang J, Feng L *et al*. Poly-ADP ribosylation of PTEN by tankyrases promotes PTEN degradation and tumor growth. Genes & development. 2015; 29: 157-170.
30. Hu K, Wu W, Li Y, Lin L, Chen D, Yan H *et al*. Poly(ADP-ribosyl)ation of BRD7 by

PARP1 confers resistance to DNA-damaging chemotherapeutic agents. EMBO reports. 2019; 20.

31. Shen J, Yu Z, Li N. The E3 ubiquitin ligase RNF146 promotes colorectal cancer by activating the Wnt/β-catenin pathway via ubiquitination of Axin1. Biochemical and biophysical research communications. 2018; 503: 991-997.
32. Wang H, Lu B, Castillo J, Zhang Y, Yang Z, McAllister G *et al*. Tankyrase Inhibitor Sensitizes Lung Cancer Cells to Endothelial Growth Factor Receptor (EGFR) Inhibition via Stabilizing Angiomotins and Inhibiting YAP Signaling. The Journal of biological chemistry. 2016; 291: 15256-15266.
33. Gao Y, Song C, Hui L, Li CY, Wang J, Tian Y *et al*. Overexpression of RNF146 in non-small cell lung cancer enhances proliferation and invasion of tumors through the Wnt/β-catenin signaling pathway. PloS one. 2014; 9: e85377.
34. Biederstädt A, Hassan Z, Schneeweis C, Schick M, Schneider L, Muckenhuber A *et al*. SUMO pathway inhibition targets an aggressive pancreatic cancer subtype. Gut. 2020; 69: 1472-1482.
35. Zhang XW, Yan XJ, Zhou ZR, Yang FF, Wu ZY, Sun HB *et al*. Arsenic trioxide controls the fate of the PML-RARalpha oncoprotein by directly binding PML. Science (New York, NY). 2010; 328: 240-243.
36. Streich FC, Jr., Lima CD. Capturing a substrate in an activated RING E3/E2-SUMO complex. Nature. 2016; 536: 304-308.
37. Yunus AA, Lima CD. Structure of the Siz/PIAS SUMO E3 ligase Siz1 and determinants required for SUMO modification of PCNA. Molecular cell. 2009; 35: 669-682.
38. Zhao W, Zhang X, Rong J. SUMOylation as a Therapeutic Target for Myocardial Infarction. Frontiers in cardiovascular medicine. 2021; 8: 701583.
39. Vertegaal ACO. Signalling mechanisms and cellular functions of SUMO. Nat Rev Mol Cell Biol. 2022.
40. Huang SM, Mishina YM, Liu S, Cheung A, Stegmeier F, Michaud GA *et al*. Tankyrase inhibition stabilizes axin and antagonizes Wnt signalling. Nature. 2009; 461: 614-620.
41. Liu C, Li Y, Semenov M, Han C, Baeg GH, Tan Y *et al*. Control of beta-catenin phosphorylation/degradation by a dual-kinase mechanism. Cell. 2002; 108: 837-847.
42. van Veelen W, Le NH, Helvensteijn W, Blonden L, Theeuwes M, Bakker ER *et al*. β-catenin tyrosine 654 phosphorylation increases Wnt signalling and intestinal tumorigenesis. Gut. 2011; 60: 1204-1212.
43. Saxena S, Zou L. Hallmarks of DNA replication stress. Molecular Cell. 2022; 82: 2298-2314.
44. Dagg RA, Zonderland G, Lombardi EP, Rossetti GG, Groelly FJ, Barroso S *et al*. A transcription-based mechanism for oncogenic beta-catenin-induced lethality in BRCA1/2-deficient cells. Nat Commun. 2021; 12: 4919.
45. Zhao Q, Xie Y, Zheng Y, Jiang S, Liu W, Mu W *et al*. GPS-SUMO: a tool for the prediction of sumoylation sites and SUMO-interaction motifs. Nucleic Acids Res. 2014; 42: W325-330.

46. Beauclair G, Bridier-Nahmias A, Zagury JF, Saib A, Zamborlini A. JASSA: a comprehensive tool for prediction of SUMOylation sites and SIMs. Bioinformatics. 2015; 31: 3483-3491.
47. Sharma A, Lysenko A, López Y, Dehzangi A, Sharma R, Reddy H *et al*. HseSUMO: Sumoylation site prediction using half-sphere exposures of amino acids residues. BMC Genomics. 2019; 19.
48. Du Y, Hou G, Zhang H, Dou J, He J, Guo Y *et al*. SUMOylation of the m6A-RNA methyltransferase METTL3 modulates its function. Nucleic Acids Res. 2018; 46: 5195-5208.
49. Cong F, Varmus H. Nuclear-cytoplasmic shuttling of Axin regulates subcellular localization of beta-catenin. Proc Natl Acad Sci U S A. 2004; 101: 2882-2887.
50. Hsiao SJ, Smith S. Tankyrase function at telomeres, spindle poles, and beyond. Biochimie. 2008; 90: 83-92.
51. Chandrakumar AA, Coyaud E, Marshall CB, Ikura M, Raught B, Rottapel R. Tankyrase regulates epithelial lumen formation via suppression of Rab11 GEFs. J Cell Biol. 2021; 220.
52. Hu K, Li Y, Wu W, Xie L, Yan H, Cai Y *et al*. ATM-Dependent Recruitment of BRD7 is required for Transcriptional Repression and DNA Repair at DNA Breaks Flanking Transcriptional Active Regions. Adv Sci (Weinh). 2020; 7: 2000157.
53. Varejao N, Ibars E, Lascorz J, Colomina N, Torres-Rosell J, Reverter D. DNA activates the Nse2/Mms21 SUMO E3 ligase in the Smc5/6 complex. EMBO J. 2018; 37.

Fig. 1 RNF146 is SUMOylated by SUMO3 at lysine 19, lysine 61, and lysine 174/175. A HeLa cells stably expressing SFB-tagged RNF146 (SFP-RNF146) or the SFB-tagged vector were transfected with HA-SUMO1, HA-SUMO2 or HA-SUMO3 for 24 h. The harvested cells were lysed with NETN buffer and subjected to immunoprecipitation (IP) and Western blotting with indicated antibodies. **B** HeLa cells stably expressing SFB-RNF146 or SFB-tagged vector were transfected with HA-SUMO3 for 24 h, and the cell lysates were then subjected to IP using anti-HA beads and detected with the indicated antibodies. **C** HeLa cells stably overexpressing SFB-RNF146 were transfected with either the scrambled or UBC9 siRNA for 48 h and were then transfected HA-SUMO3 for 24 h. The cells were harvested and subjected to IP using anti-S beads prior to Western blot analysis. **D** HeLa cells stably expressing SFB-RNF146 or the SFB-tagged vector were transfected with HA-SUMO3 for 24 h and were then treated with 100 μM 2-D08 for 24 h. Cell lysates were then analysed as indicated. **E** HeLa cells were cotransfected with the indicated SFB-RNF146 plasmids and HA-SUMO3 for 24 h. Then, the cell lysates were subjected to IP using anti-S beads and Western blotting with the indicated antibodies**. F** Alignment of the SUMOylation sites at RNF146 in different species.

Fig. 2 PIAS3 and MMS21 are the dominant SUMO E3 ligases for RNF146. A HeLa cells stably expressing SFB-RNF146 were cotransfected with HA-SUMO3 and each plasmid expressing the indicated 3MYC-tagged PIAS family members for 24 h. The harvested cells were lysed with NETN buffer, and subjected to IP using anti-S beads and Western blotting. **B** HeLa cells stably expressing SFB-RNF146 were transiently cotransfected with HA-SUMO3 and either 3MYC- tagged PIAS3 or 3MYC- tagged MMS21 for 24 h. Then, whole-cell lysates were subjected to IP using anti-MYC beads and detection with the indicated antibodies. **C** HeLa cells were lysed with RIPA buffer, and whole-cell lysates were subjected to co-IP using IgG or an

anti-RNF146 antibody and analysed by Western blotting. **D** SK-hep1 cells were cotransfected with mCherry-RNF146 and V5-turbo-PIAS3/MMS21 for 36 h. After fixation, immunofluorescence staining was performed using the indicated antibody and DAPI; the scale bar indicates 10 μm. **E, F** HeLa cells stably overexpressing SFB-RNF146 were transfected with HA-SUMO3 for 24 h prior to treatment with scrambled siRNA and either the PIAS3 (E) or MMS21 (F) siRNAs for another 48 h. The cells were harvested and subjected to IP using the indicated antibodies. **G** HeLa cells stably overexpressing SFB-RNF146 were transfected with scrambled， PIAS3, MMS21 or PIAS3/MMS21 siRNAs for 48 h and lysed with NETN buffer, prior to IP and Western blot analysis with the indicated antibodies.

Fig. 3 SENP1/2/6 are the dominant deSUMOylases responsible for removing SUMOylation from RNF146. A HeLa cells stably expressing SFB-RNF146 were cotransfected with HA-SUMO3 and each plasmid expressing the indicated 3MYC-tagged SENP family members for 24 h. The harvested cells were lysed with NETN buffer and subjected to IP using anti-S beads and Western blotting using the indicated antibodies. **B** HeLa cells overexpressing SFB-RNF146 were transiently cotransfected with HA-SUMO3 and 3MYC-tagged SENP1/2/6 for 24 h, and whole-cell lysates were then subjected to IP using anti-MYC beads and detection with the indicated antibodies. **C** HeLa cell lysates were incubated with protein-G agarose beads conjugated to IgG or an anti-RNF146 antibody; the results of an IP assay are shown. **D** 293T and SK-hep1 cells were cotransfected with mCherry-RNF146 and V5-turbo-SENP1 for 36 h. Then, the cells were fixed and stained with the indicated antibodies and DAPI. The scale bar represents 10 μm. **E** SFB-RNF146 stably overexpressing HeLa cells were transfected with scrambled and siRNAs for SENP1 for 48 h, and then transfected with HA-SUMO3 for another 24 h. After being lysed with NETN buffer, cell lysates were analyzed by IP and Western blot using indicated antibodies. **F** HeLa cells

stably expressing SFB-RNF146 were transfected with scrambled, SENP1, SENP2, SENP6 or SENP1/SENP2/SENP6 siRNAs for 48 h and then transfected with HA-SUMO3 for another 24 h. Cell lysates were harvested and subjected to IP using anti-S beads prior to Western blot analysis.

Fig. 4 SUMOylation of RNF146 at lysine 19 and lysine 175 promotes the interaction of RNF146 with Axin and the degradation of Axin. A Endogenous RNF146 was knocked out with sgRNA, and SFB-vector or the indicated SFB-RNF146 mutation plasmids were then transfected into SK-hep1 cells for 24 h. The expression of the indicated proteins was determined by Western blotting. **B** Cytoplasmic and nuclear distribution of β-catenin and SFB-RNF146 in SK-hep1 cells stably expressing SFB-vector or SFB-RNF146. **C** Endogenous RNF146 was depleted in SK-hep1 cells. The cytoplasmic and nuclear distribution of β-catenin was analysed after transfection with SFB-vector or the indicated SFB-RNF146 plasmids. **D** SK-hep1 cells stably expressing SFB-RNF146 were treated with scrambled siRNA or siRNAs for PIAS3 and MMS21 for 72 h. Then, the cells were lysed with RIPA buffer, and the expression of Axin and β-catenin was analysed by Western blotting. **E** SK-hep1 cells stably expressing SFB-RNF146 were treated with scrambled siRNA or siRNAs for SENP1, SENP2 or SENP6 for 72 h. The expression of Axin and β-catenin were analysed by Western blotting. **F** SK-hep1 cells with depletion of endogenous RNF146 and stab expression of SFB-vector, wild-type SFB-RNF146 or mutant SFB-RNF146 plasmids were lysed with NETN buffer. Then, whole-cell lysates were subjected to IP using anti-S beads and analysed by Western blotting to evaluate the interaction between RNF146 and Axin. **G** SK-hep1 cells with depletion of endogenous RNF146 and stable expression of SFB-vector, wild-type SFB-RNF146 or mutant SFB-RNF146 plasmids were transfected with HA-Ub for 24 h. Cell lysates were subjected to co-IP using an anti-Axin antibody, and Western blotting was performed using the indicated antibodies.

Fig. 5 RNF146 SUMOylation activates β-catenin signaling and promotes the proliferation of HCC cells in vitro. A SFB-vector and SFB-RNF146 overexpression plasmids were stably transfected into SK-hep1 and HCC-LM3 cells. Axin and β-catenin signaling was analysed by Western blotting using the indicated antibodies. **B** RNF146 was knocked out with two sgRNAs in SK-hep1 and HCC-LM3 cells. Cell lysates were analysed by Western blotting using the indicated antibodies. **C** The proliferative ability of SK-hep1 and HCC-LM3 cells stably expressing SFB-vector or SFB-RNF146 was determined by the colony formation assay. n = 3 independent experiments. **D** SK-hep1 and HCC-LM3 cells with stable depletion of RNF146 were subjected to the colony formation assay. n = 3 independent experiments. **E, F** SK-hep1 or HCC-LM3 cells with stable overexpression (E) or depletion (F) of RNF146 were sequentially labelled with IdU and CldU for 20 min. Three independent experiments were performed, and the replication fork speed was calculated and analysed. **G** The SFB-vector, SFB-RNF146 wild-type and SFB-RNF146 mutant plasmids were stably expressed in SK-hep1 and HCC-LM3 cells in which endogenous RNF146 was depleted by sgRNA. Three independent experiments were performed, and the percentage of BrdU-positive cells was quantified and analysed. **H** The indicated stable cell lines were subjected to a colony formation assay. n = 3 independent experiments. **I, J** SK-hep1 and HCC-LM3 stable cell lines were used, and the DNA fiber assay was performed. Representative images are shown in (I). The replication fork speed was quantified and analysed as shown in (J). n = 3 independent experiments. n. s, not significant; *$p < 0.05$; **$p < 0.01$; ***$p < 0.001$.

Fig. 6 Abolishing RNF146 SUMOylation inhibits HCC cell tumorigenesis. A SK-hep1 cells with depletion of endogenous RNF146 and stable expression of SFB-vector, SFB-RNF146-WT or SFB-RNF146-mutants were injected into the flanks of nude mice. Tumour growth was measured every 2 days. **B, C**

Harvested xenografts were photographed (B) and weighed (C). **D** The expression of Axin and β-catenin in xenografts was analysed by Western blotting. **E** IHC staining of harvested xenografts using antibodies against Ki67, RNF146 and Axin. The scale bar indicates 100 μm. **F, G** SK-hep1 cells were injected into the flanks of nude mice. Six days after injection, the mice were intraperitoneally injected with 2-D08 (5 mg/kg) or vehicle (10% DMSO, 40% PEG300, 5% Tween 80, 45% saline) every 2 days. Tumour growth (F) and weight (G) were measured as indicated. n. s, not significant; *$p < 0.05$; ***$p < 0.001$.

Fig. 7 The clinical significance of RNF146 SUMOylation/Axin/β-catenin axis in human HCC tissues. A, B The expression of RNF146, UBC9, PIAS3 and SENP1 in HCC tumor and adjacent specimens (n = 12) was analyzed by Western blotting using indicated antibodies (A), and their expression were quantified and analysed as shown in (B). **C** Representative IHC images of RNF146, Axin, PIAS3 and SENP1 staining using HCC tissues. Scale bar indicates 100 μm. **D** The association between Axin expression and UBC9, RNF146, PIAS3 or SENP1（n = 99). The percentage of positive staining and *p* value based on Pearson's χ^2 test and Pearson's correlations are shown in the tables. **E** UBC9 expression in HCC (n = 369) and non-tumour tissues (n = 50) analyzed by the GEPIA2 web tool. **F** The correlation between the expression pattern of RNF146 and UBC9 with the overall survival of HCC patients was analyzed using data from TCGA. The high and low grouping of RNF146 and UBC9 was based on the median of the gene expression. n. s, not significant; *$p < 0.05$; **$p < 0.01$; ***$p < 0.001$.

Fig. 8 Schematic model of the SUMO-RNF146-Axin pathway. PIAS3-mediated SUMOylation of RNF146 promotes its translocation from the cytoplasm to the nucleus, while deSUMOylation of RNF146 is catalysed by

SENP1, facilitating its nuclear export. SUMOylation of RNF146 promotes its association with Axin and accelerates Axin ubiquitination and degradation, thereby activating β-catenin signaling and resulting in HCC progression.

Figures

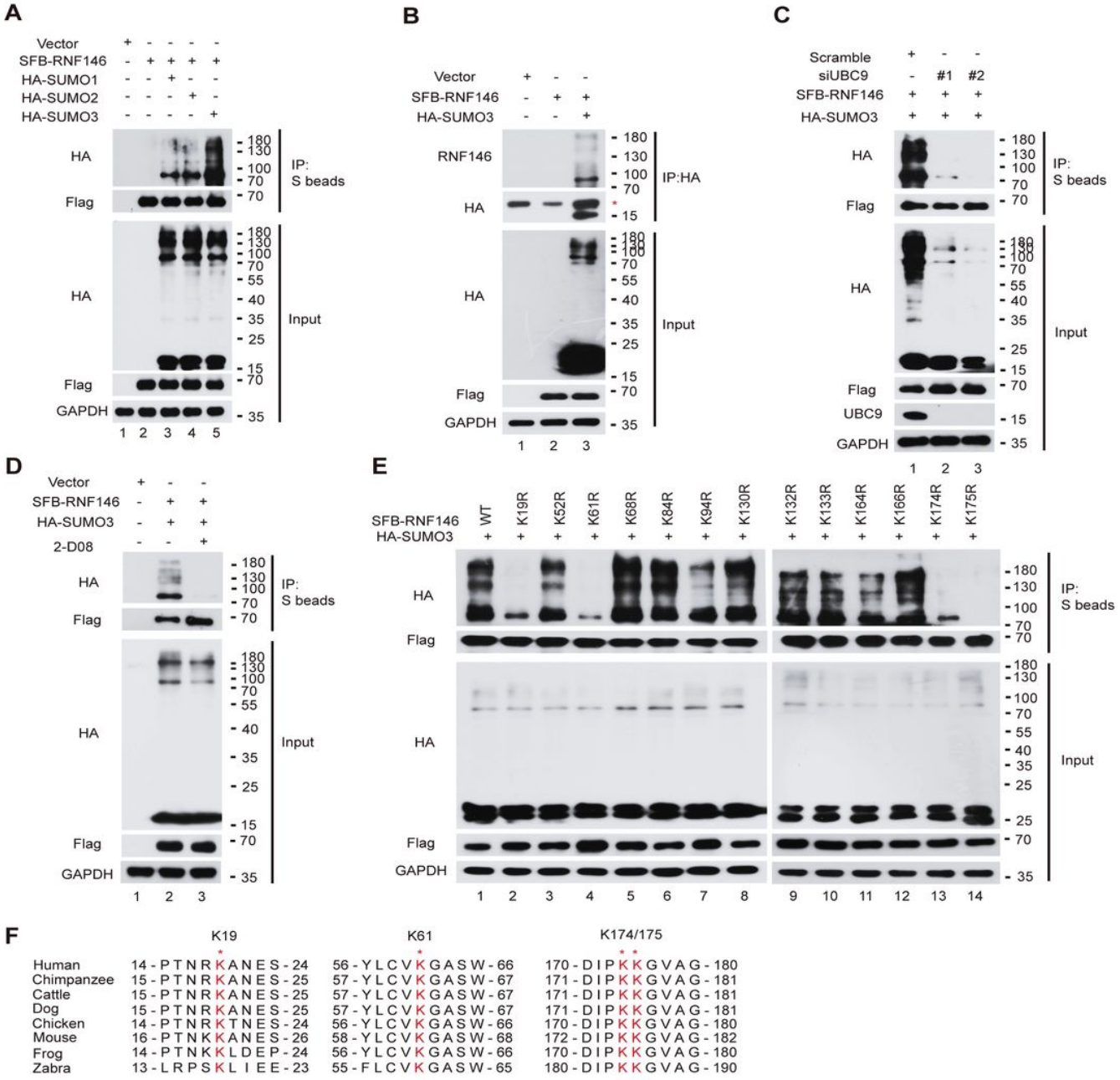

Figure 1

RNF146 is SUMOylated by SUMO3 at lysine 19, lysine 61, and lysine 174/175. A HeLa cells stably expressing SFB-tagged RNF146 (SFP-RNF146) or the SFB-tagged vector were transfected with HA-SUMO1, HA-SUMO2 or HA-SUMO3 for 24 h. The harvested cells were lysed with NETN buffer and subjected to immunoprecipitation (IP) and Western blotting with indicated antibodies. B HeLa cells stably expressing SFB-RNF146 or SFB-tagged vector were transfected with HA-SUMO3 for 24 h, and the cell lysates were then subjected to IP using anti-HA beads and detected with the indicated antibodies. C HeLa cells stably overexpressing SFB-RNF146 were transfected with either the scrambled or UBC9 siRNA for 48 h and were then transfected HA-SUMO3 for 24 h. The cells were harvested and subjected to IP using anti-

S beads prior to Western blot analysis. D HeLa cells stably expressing SFB-RNF146 or the SFB-tagged vector were transfected with HA-SUMO3 for 24 h and were then treated with 100 μM 2-D08 for 24 h. Cell lysates were then analysed as indicated. E HeLa cells were cotransfected with the indicated SFB-RNF146 plasmids and HA-SUMO3 for 24 h. Then, the cell lysates were subjected to IP using anti-S beads and Western blotting with the indicated antibodies. F Alignment of the SUMOylation sites at RNF146 in different species.

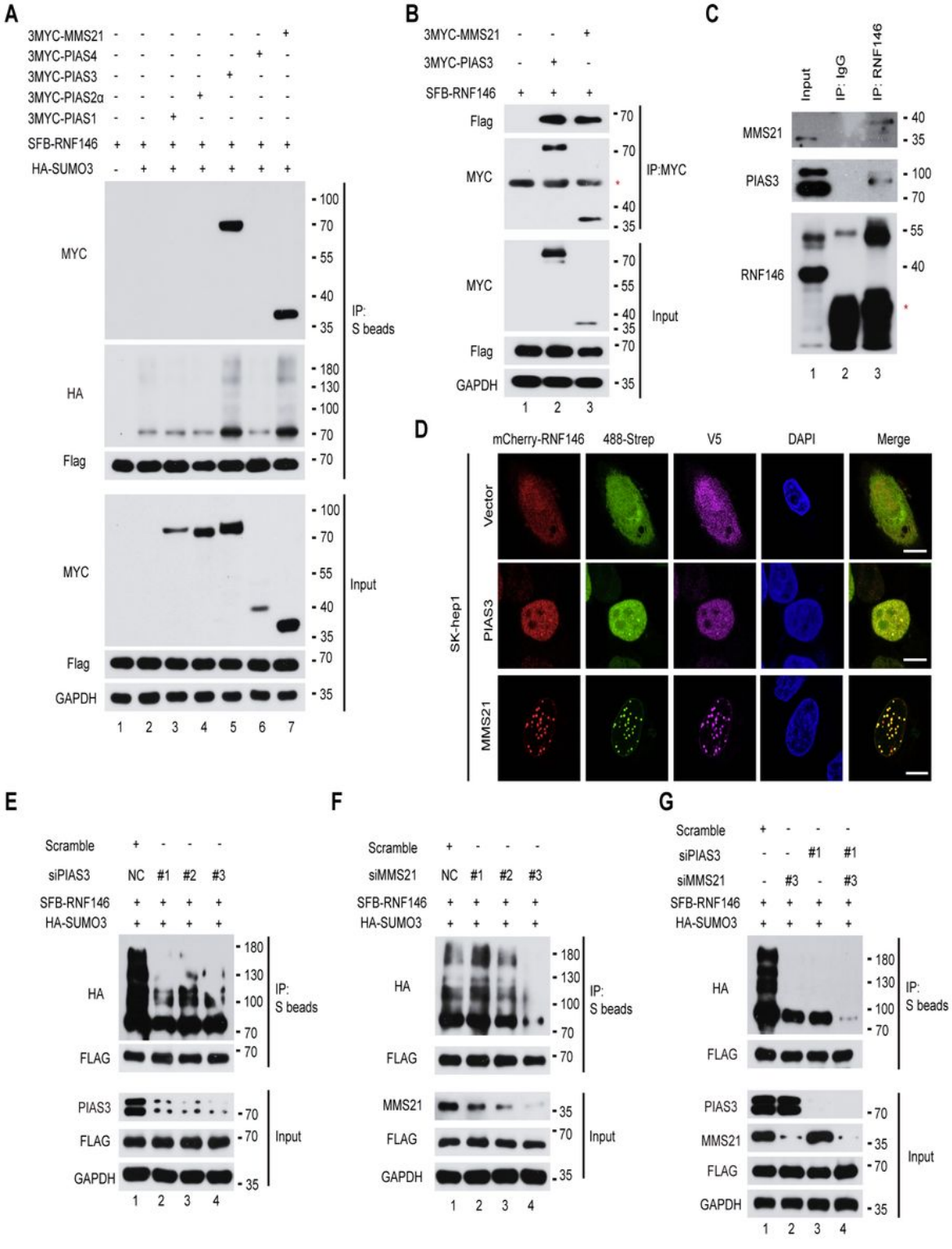

Figure 2

PIAS3 and MMS21 are the dominant SUMO E3 ligases for RNF146. A HeLa cells stably expressing SFB-RNF146 were cotransfected with HA-SUMO3 and each plasmid expressing the indicated 3MYC-tagged PIAS family members for 24 h. The harvested cells were lysed with NETN buffer, and subjected to IP using anti-S beads and Western blotting. B HeLa cells stably expressing SFB-RNF146 were transiently cotransfected with HA-SUMO3 and either 3MYC- tagged PIAS3 or 3MYC- tagged MMS21 for 24h. Then, whole-cell lysates were subjected to IP using anti-MYC beads and detection with the indicated antibodies. C HeLa cells were lysed with RIPA buffer, and whole-cell lysates were subjected to co-IP using IgG or an anti-RNF146 antibody and analysed by Western blotting. 710 D SK-hep1 cells were cotransfected with mCherry-RNF146 and V5-turbo-PIAS3/MMS21 for 36h. After fixation, immunofluorescence staining was performed using the indicated antibody and DAPI; the scale bar indicates 10 μm. E, F HeLa cells stably overexpressing SFB-RNF146 were transfected with HA-SUMO3 for 24h prior to treatment with scrambled siRNA and either the PIAS3 (E) or MMS21 (F) siRNAs for another 48 h. The cells were harvested and subjected to IP using the indicated antibodies. G HeLa cells stably overexpressing SFB-RNF146 were transfected with scrambled PIAS3, MMS21 or PIAS3/MMS21 siRNAs for 48 h and lysed with NETN buffer, prior to IP and Western blot analysis with the indicated antibodies.

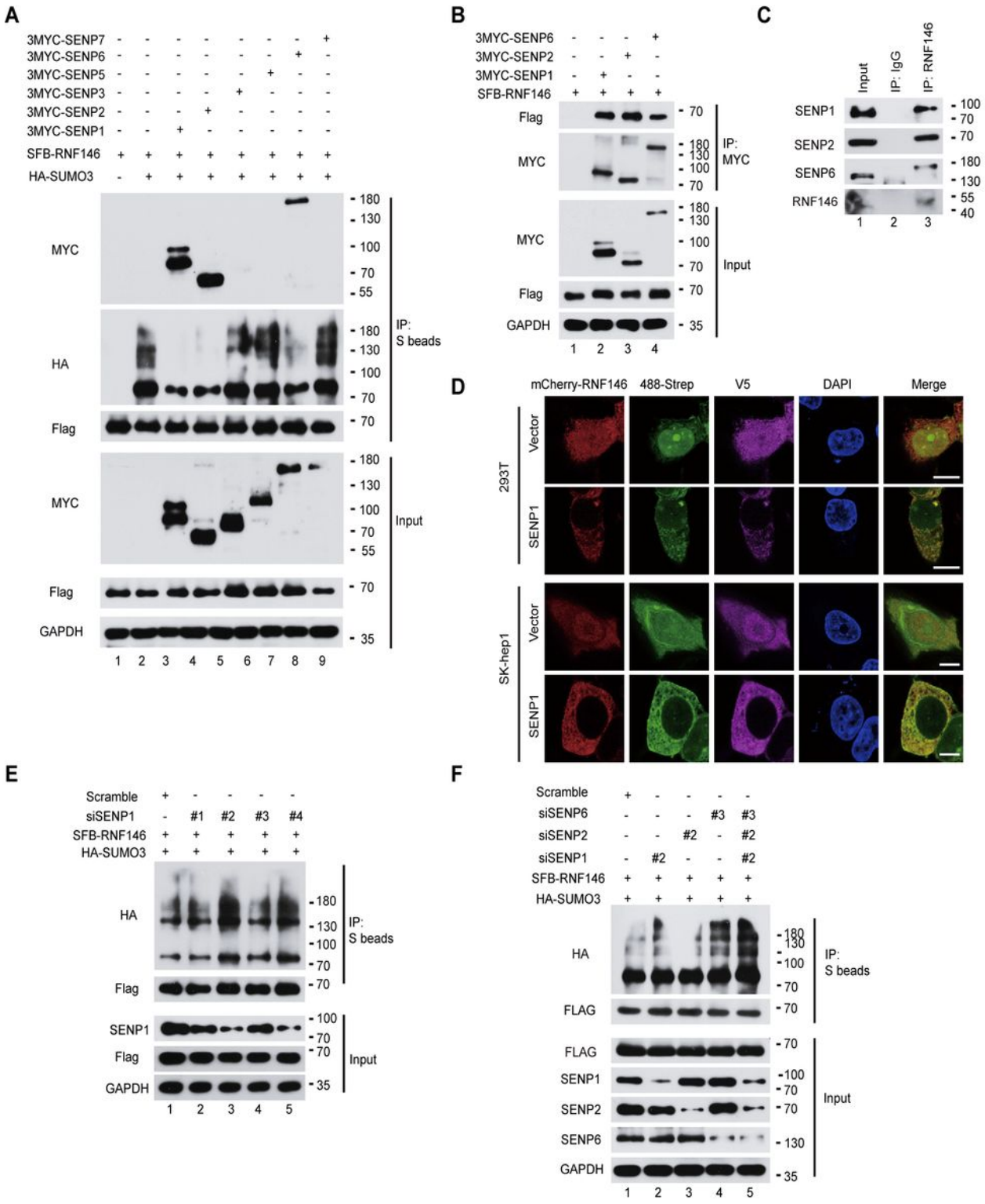

Figure 3

SENP1/2/6 are the dominant deSUMOylases responsible for removing SUMOylation from RNF146. A HeLa cells stably expressing SFB-RNF146 were cotransfected with HA-SUMO3 and each plasmid expressing the indicated 3MYC-tagged SENP family members for 24 h. The harvested cells were lysed with NETN buffer and subjected to IP using anti-S beads and Western blotting using the indicated antibodies. B HeLa cells overexpressing SFB-RNF146 were transiently cotransfected with HA-SUMO3 and

3MYC-tagged SENP1/2/6 for 24 h, and whole-cell lysates were then subjected to IP using anti-MYC beads and detection with the indicated antibodies. C HeLa cell lysates were incubated with protein-G agarose beads conjugated to IgG or an anti-RNF146 antibody; the results of an IP assay are shown. D 293T and SK-hep1 cells were cotransfected with mCherry-RNF146 and V5-turbo-SENP1 for 36 h. Then, the cells were fixed and stained with the indicated antibodies and DAPI. The scale bar represents 10 μm. E SFB-RNF146 stably overexpressing HeLa cells were transfected with scrambled and siRNAs for SENP1 for 48 h, and then transfected with HA-SUMO3 for another 24 h. After being lysed with NETN buffer, cell lysates were analyzed by IP and Western blot using indicated antibodies. F HeLa cells stably expressing SFB-RNF146 were transfected 740 with scrambled, SENP1, SENP2, SENP6 or SENP1/SENP2/SENP6 siRNAs for 48 h and then transfected with HA-SUMO3 for another 24 h. Cell lysates were harvested and subjected to IP using anti-S beads prior to Western blot analysis.

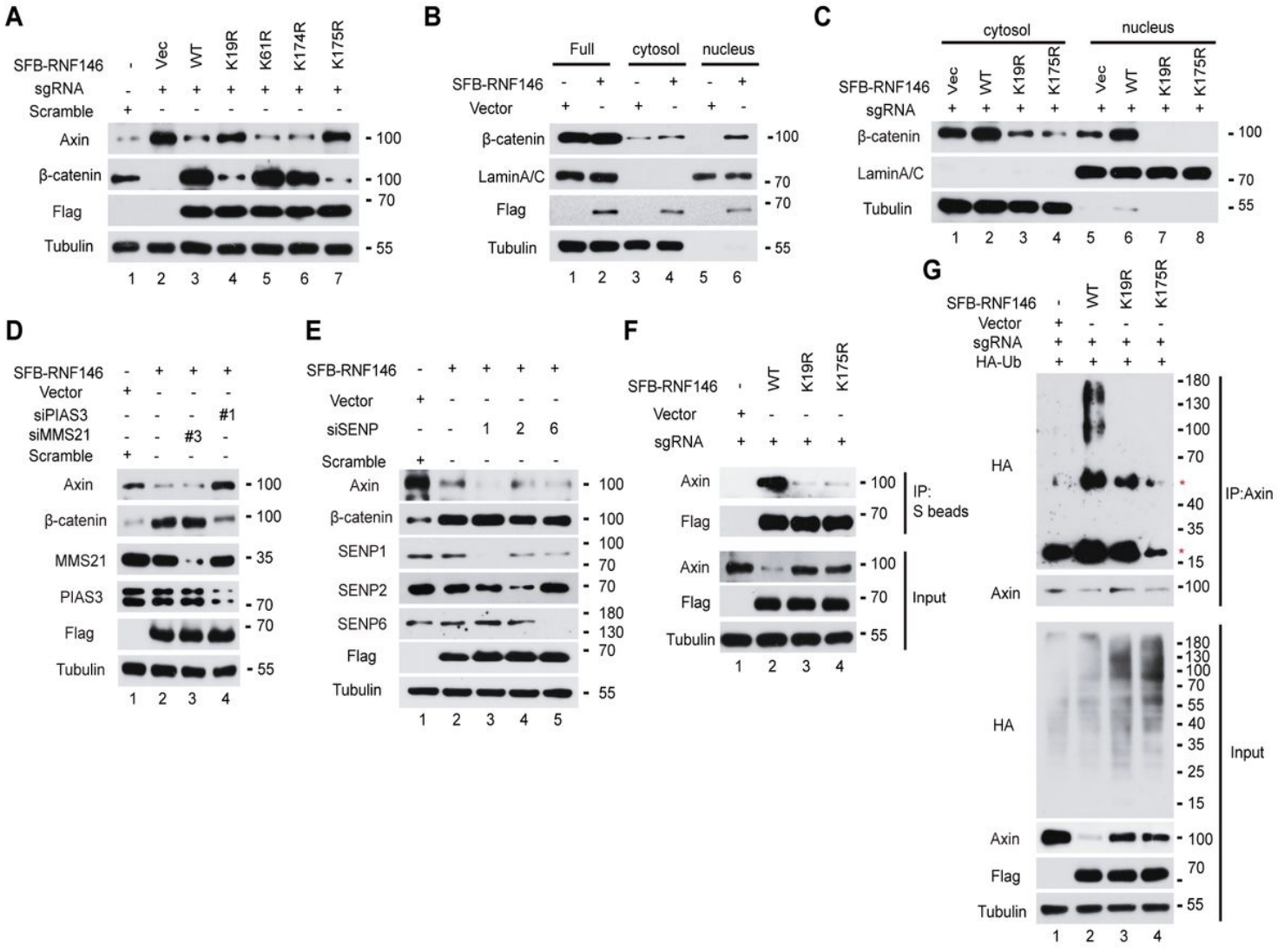

Figure 4

SUMOylation of RNF146 at lysine 19 and lysine 175 promotes the interaction of RNF146 with Axin and the degradation of Axin. A Endogenous RNF146 was knocked out with sgRNA, and SFB-vector or the

indicated SFB-RNF146 mutation plasmids were then transfected into SK-hep1 cells for 24 h. The expression of the indicated proteins was determined by Western blotting. B Cytoplasmic and nuclear distribution of β-catenin and SFB-RNF146 in SK-hep1 cells stably expressing SFB-vector or SFB-RNF146. C Endogenous RNF146 was depleted in SK-hep1 cells. The cytoplasmic and nuclear distribution of β-catenin was analysed after transfection with SFB-vector or the indicated SFB-RNF146 plasmids. D SK-hep1 cells stably expressing SFB-RNF146 were treated with scrambled siRNA or siRNAs for PIAS3 and MMS21 for 72 h. Then, the cells were lysed with RIPA buffer, and the expression of Axin and β-catenin was analysed by Western blotting. E SK-hep1 cells stably expressing SFB-RNF146 were treated with scrambled siRNA or siRNAs for SENP1, SENP2 or SENP6 for 72 h. The expression of Axin and β-catenin were analysed by Western blotting. F SK-hep1 cells with depletion of endogenous RNF146 and stab expression of SFB-vector, wild-type SFB-RNF146 or mutant SFB-RNF146 plasmids were lysed with NETN buffer. Then, whole-cell lysates were subjected to IP using anti-S beads and analysed by Western blotting to evaluate the interaction between RNF146 and Axin. G SK-hep1 cells with depletion of endogenous RNF146 and stable expression of SFB-vector, wild-type SFB-RNF146 or mutant SFB-RNF146 plasmids were transfected with HA-Ub for 24 h. Cell lysates were subjected to co-IP using an anti-Axin antibody, and Western blotting was performed using the indicated antibodies.

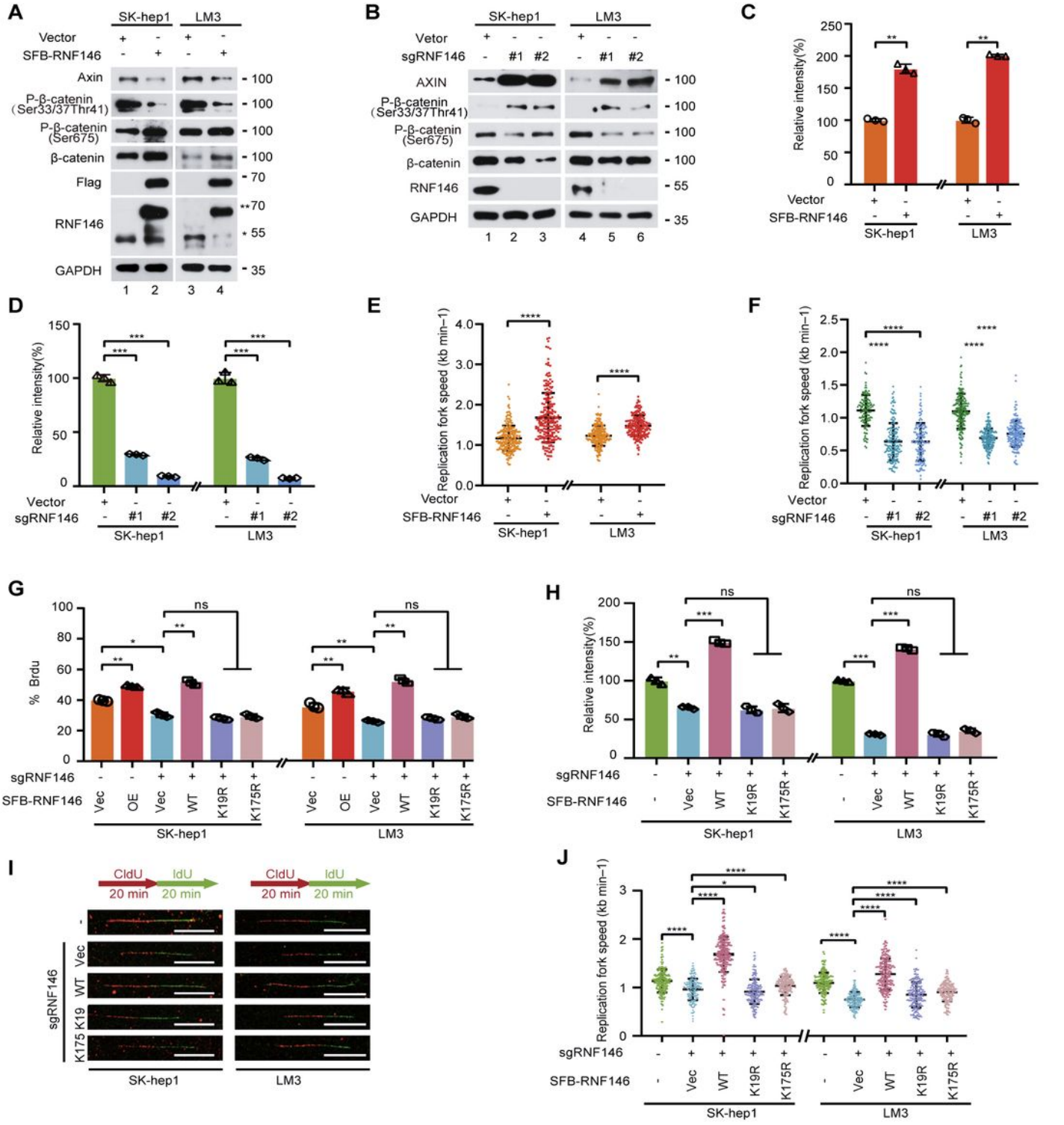

Figure 5

RNF146 SUMOylation activates β-catenin signaling and promotes the proliferation of HCC cells in vitro. A SFB-vector and SFB-RNF146 overexpression plasmids were stably transfected into SK-hep1 and HCC-LM3 cells. Axin and β-catenin signaling was analysed by Western blotting using the indicated antibodies. B RNF146 was knocked out with two sgRNAs in SK-hep1 and HCC-LM3 cells. Cell lysates were analysed by Western blotting using the indicated antibodies. C The proliferative ability of SK-hep1 and HCC-LM3

cells stably expressing SFB-vector or SFB-RNF146 was determined by the colony formation assay. n = 3 independent experiments. D SK-hep1 and HCC-LM3 cells with stable depletion of RNF146 were subjected to the colony formation assay. n = 3 independent experiments. E, F SK-hep1 or HCC-LM3 cells with stable overexpression (E) or depletion (F) of RNF146 were sequentially labelled with IdU and CldU for 20 min. Three independent experiments were performed, and the replication fork speed was calculated and analysed. G The SFB-vector, SFB-RNF146 wild-type and SFB-RNF146 mutant plasmids were stably expressed in SK-hep1 and HCC-LM3 cells in which endogenous RNF146 was depleted by sgRNA. Three independent experiments were performed, and the percentage of BrdU-positive cells was quantified and analysed. H The indicated stable cell lines were subjected to a colony formation assay. n = 3 independent experiments. I, J SK-hep1 and HCC-LM3 stable cell lines were used, and the DNA fiber assay was performed. Representative images are shown in (I). The replication fork speed was quantified and analysed as shown in (J). n = 3 independent experiments. n. s, not significant; *p < 0.05; **p < 0.01; ***p < 0.001.

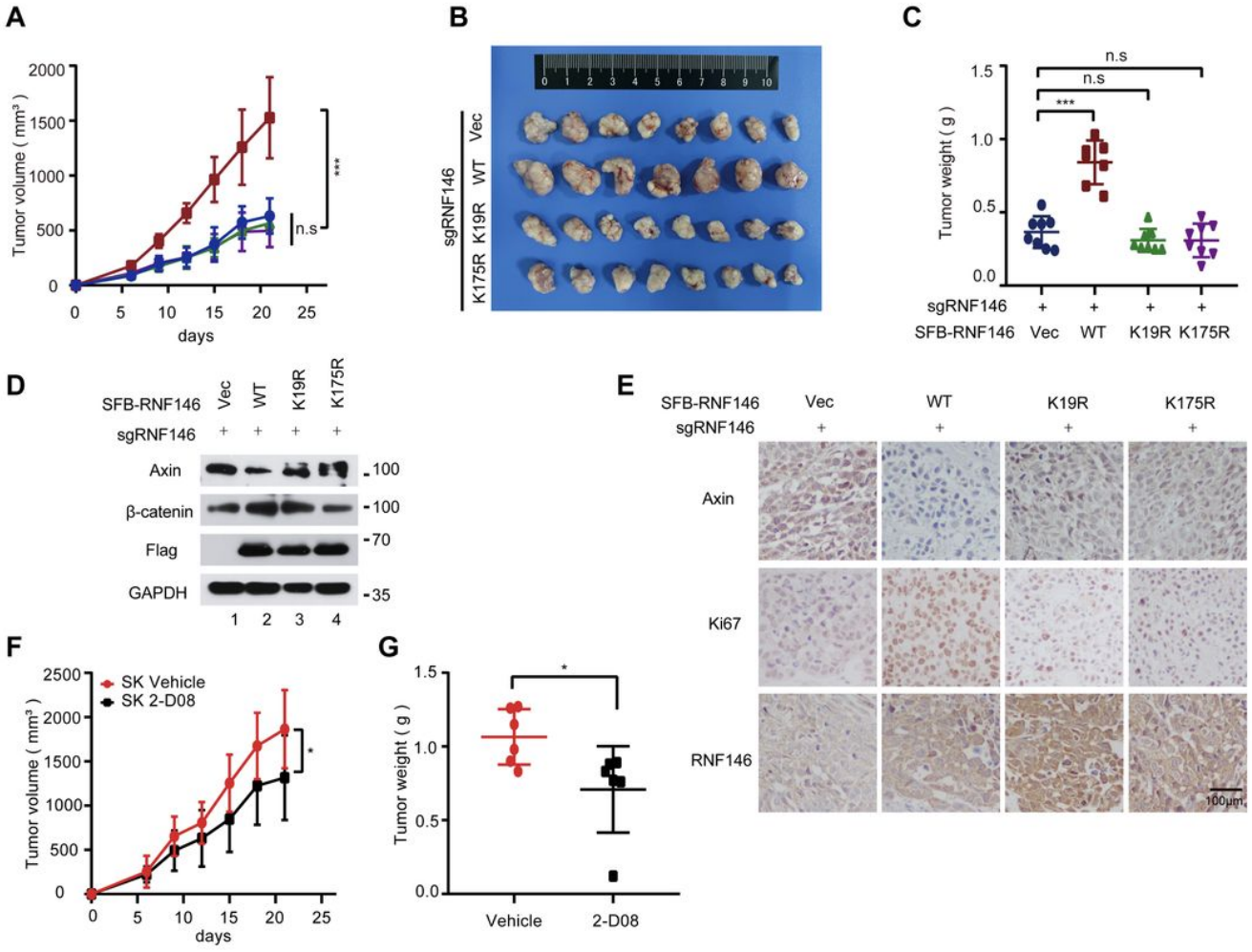

Figure 6

Abolishing RNF146 SUMOylation inhibits HCC cell tumorigenesis. A SK-hep1 cells with depletion of endogenous RNF146 and stable expression of SFB-vector, SFB-RNF146-WT or SFB-RNF146-mutants were

injected into the flanks of nude mice. Tumour growth was measured every 2 days. B, C Harvested xenografts were photographed (800 B) and weighed (C). D The expression of Axin and β-catenin in xenografts was analysed by Western blotting. E IHC staining of harvested xenografts using antibodies against Ki67, RNF146 and Axin. The scale bar indicates 100 μm. F, G SK-hep1 cells were injected into the flanks of nude mice. Six days after injection, the mice were intraperitoneally injected with 2-D08 (5 mg/kg) or vehicle (10% DMSO, 40% PEG300, 5% Tween 80, 45% saline) every 2 days. Tumour growth (F) and weight (G) were measured as indicated. n. s, not significant; *p < 0.05; ***p < 808 0.001.

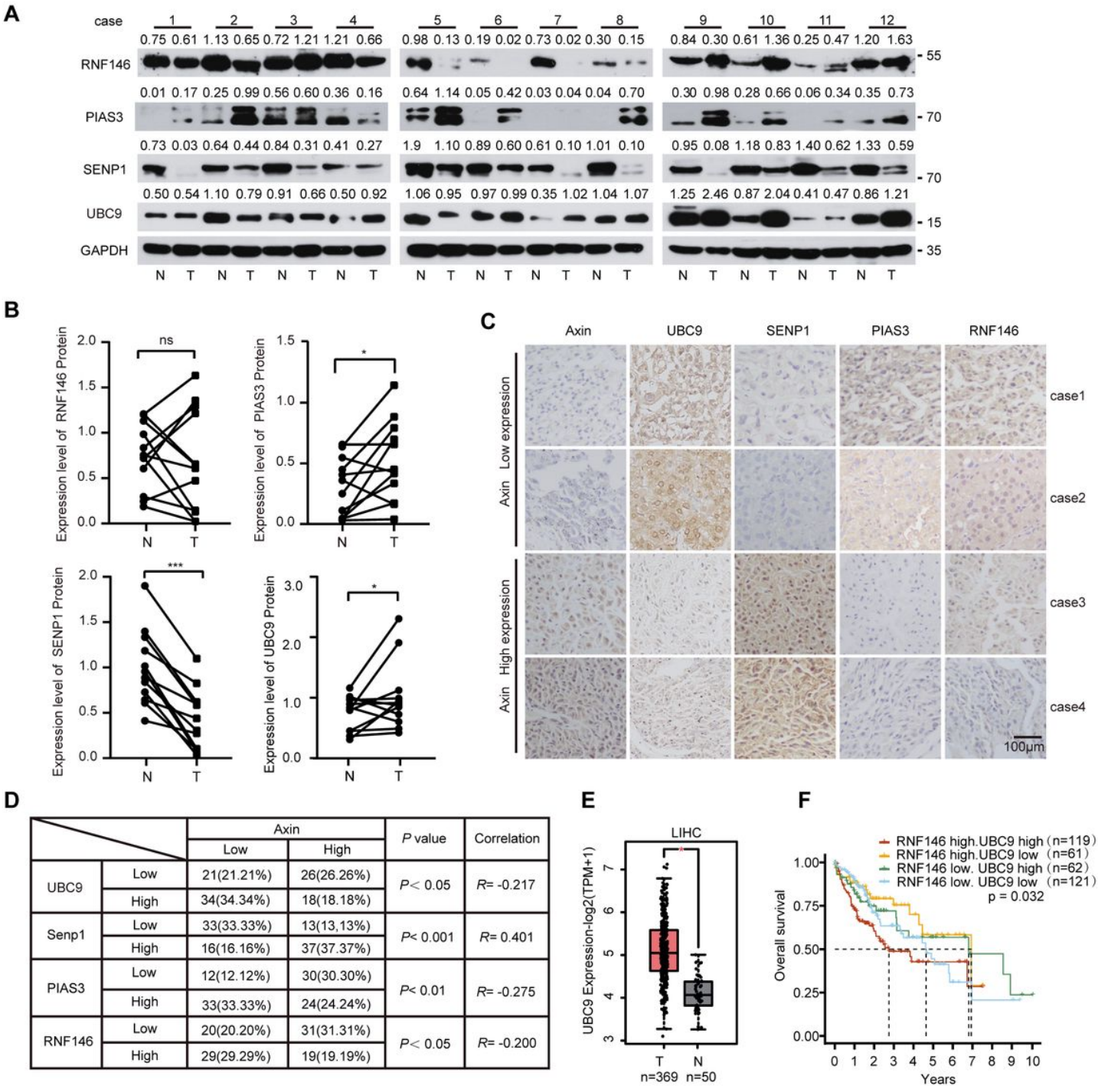

		Axin		*P* value	Correlation
		Low	High		
UBC9	Low	21(21.21%)	26(26.26%)	*P*< 0.05	*R*= -0.217
	High	34(34.34%)	18(18.18%)		
Senp1	Low	33(33.33%)	13(13,13%)	*P*< 0.001	*R*= 0.401
	High	16(16.16%)	37(37.37%)		
PIAS3	Low	12(12.12%)	30(30.30%)	*P*< 0.01	*R*= -0.275
	High	33(33.33%)	24(24.24%)		
RNF146	Low	20(20.20%)	31(31.31%)	*P*< 0.05	*R*= -0.200
	High	29(29.29%)	19(19.19%)		

Figure 7

The clinical significance of RNF146 SUMOylation/Axin/β-catenin axis in human HCC tissues. A, B The expression of RNF146, UBC9, PIAS3 and SENP1 in HCC tumor and adjacent specimens (n = 12) was analyzed by Western blotting using indicated antibodies (A), and their expression were quantified and analysed as shown in (B). C Representative IHC images of RNF146, Axin, PIAS3 and SENP1 staining using HCC tissues. Scale bar indicates 100 μm. D The association between Axin expression and UBC9, RNF146, PIAS3 or SENP1 (n = 99). The percentage of positive staining and p value based on Pearson's $\chi 2$ test and Pearson's correlations are shown in the tables. E UBC9 expression in HCC (n = 369) and non-tumour tissues (n = 50) analyzed by the GEPIA2 web tool. F The correlation between the expression pattern of RNF146 and UBC9 with the overall survival of HCC patients was analyzed using data from TCGA. The high and low grouping of RNF146 and UBC9 was based on the median of the gene expression. n. s, not significant; *$p < 0.05$; **$p < 0.01$; ***$p < 0.001$.

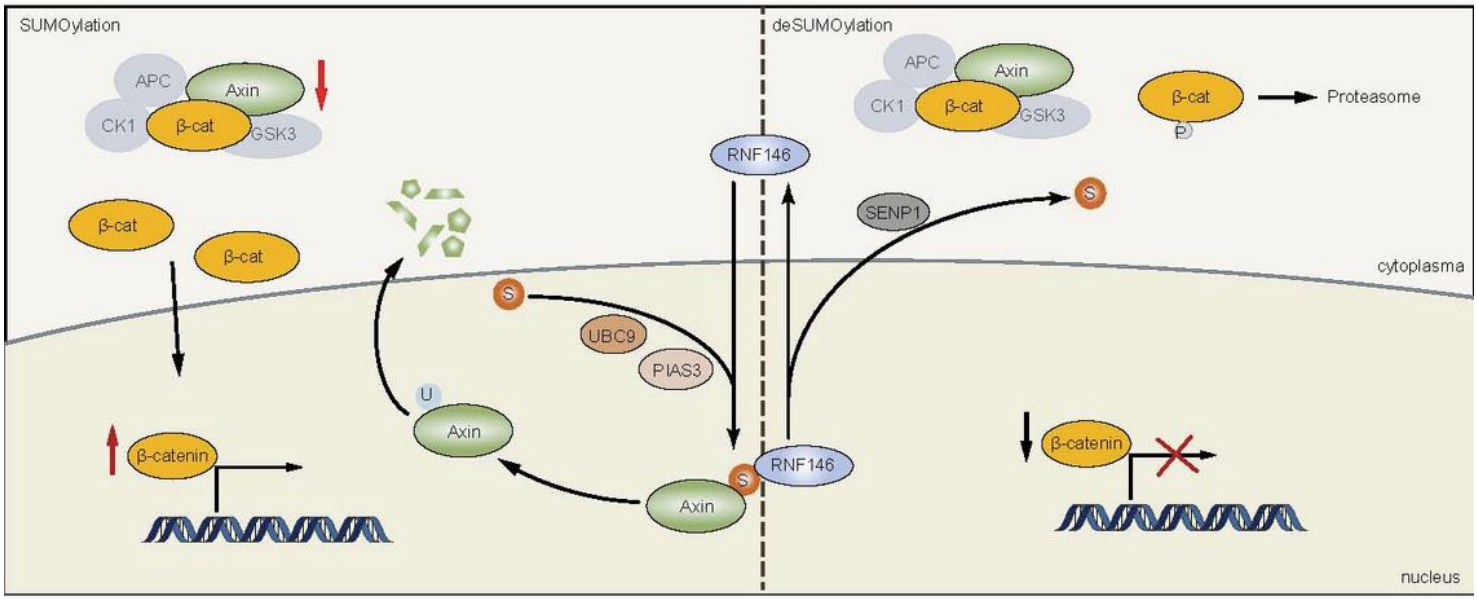

Figure 8

Schematic model of the SUMO-RNF146-Axin pathway.

PIAS3-mediated SUMOylation of RNF146 promotes its translocation from the cytoplasm to the nucleus, while deSUMOylation of RNF146 is catalysed by

SENP1, facilitating its nuclear export. SUMOylation 830 of RNF146 promotes its association with Axin and accelerates Axin ubiquitination and degradation, thereby activating β-catenin signaling and resulting in HCC progression.

Supplementary Files

This is a list of supplementary files associated with this preprint. Click to download.

- supplymentarymaterials.pdf